Subsalt event regularization with steering filters

Marie L. Prucha and Biondo L. Biondi, Stanford University*

SUMMARY

The difficulties of imaging beneath salt bodies are well known. We present an angle-domain least-squares inversion scheme that regularizes the seismic image, tending to create specified dips. This dip creation is accomplished using a non-stationary operator composed of dip filters (a steering filter). We show the results of using the regularized inversion along the angle axis and along both the angle and common midpoint axes. Additionally, the result of specifying incorrect dips is examined. The results show that this regularized least-squares inversion does produce a cleaner, more continuous result under salt bodies and the inversion will reject incorrectly chosen dips used for the regularization.

INTRODUCTION

Obtaining a clean, coherent seismic image in areas of complex subsurface can be difficult. This is particularly true when the subsurface lends itself to shadow zones, such as those under the edges of salt bodies. In these areas, little of the seismic energy gets to the reflectors, and even less energy makes it back to the surface. In addition to the shadow zones, proper imaging is made difficult by multipathing. Multipathing occurs when energy that follows different paths through the subsurface arrives at the receiver at the same time.

It is possible to eliminate artifacts caused by multipathing by imaging in the reflection angle domain via angle-domain Kirchhoff migration (Brandsberg-Dahl et al., 1999; Xu et al., 2001). However, Kirchhoff methods are not necessarily optimal for complex subsurfaces (Geoltrain and Brac, 1993; O'Brien and Etgen, 1998). To address that problem, angle-domain wave-equation migration methods have been developed (Prucha et al., 1999; Mosher and Foster, 2000; Sava et al., 2001).

Unfortunately, migration alone does not necessarily provide the best image. A better image in complex areas can often be obtained using least-squares inversion (Nemeth et al., 1999; Duquet and Marfurt, 1999). However, inversion can diverge in areas with shadow zones. Since we often have some idea of what the image in the shadow zone should look like, we can impose some sort of regularization on the inversion carried out in the angle domain (Prucha et al., 2000; Kuehl and Sacchi, 2001) to prevent these blow-ups. This regularization can be chosen as smoothing along events and therefore can be applied by the use of steering filters (Clapp, 2001). The inversion uses these steering filters to help strengthen existing events to fill in shadow zones.

In this abstract, we will first review the theory and implementation of our inversion, then show the results of three variants of this regularized inversion scheme on a fairly complex synthetic model. We will then examine the impact of the regularization operator.

THEORY

Our inversion scheme is based on the angle-domain wave-equation migration explained by Prucha et al. (1999). To summarize, this migration is carried out by downward continuing the wavefield in frequency space, slant stacking at each depth, and extracting the image at zero time. This process can be described as:

$$P(\omega,m,h;z=0) \stackrel{DSR}{\Longrightarrow} P(\omega,m,h;z) \quad (1)$$

$$P(\omega,m,h;z) \stackrel{Slant\ stack}{\Longrightarrow} P(\tau,m,p_h;z) \quad (2)$$

$$P(\tau,m,p_h;z) \stackrel{Imaging}{\Longrightarrow} P(\tau=0,m,p_h;z). \quad (3)$$

Angle-domain CIGs are subsets of $P(\tau=0,m,p_h;z)$ at fixed midpoint location. Note that the result is in offset ray parameter rather than reflection angle. This method is still considered an angle domain process because the offset ray parameter can be easily related to the reflection angle by:

$$\frac{\partial t}{\partial h} = p_h = \frac{2\sin\theta\cos\phi}{V(z,m)}, \quad (4)$$

where θ is the reflection angle, ϕ is the geologic dip, and $V(z,m)$ is the velocity function in depth and CMP location.

Wave-equation migration can be thought of as an operator and therefore used in an inversion. We choose a regularized least-squares inversion in which we minimize $Q(\mathbf{m})$:

$$Q(\mathbf{m}) = ||\mathbf{Lm}-\mathbf{d}||^2 + \epsilon^2 ||\mathbf{Am}||^2. \quad (5)$$

Here, $\mathbf{d}$ is the input data and $\mathbf{m}$ is the image obtained through inversion. $\mathbf{L}$ is a linear operator, in this case it is the adjoint of the angle-domain wave-equation migration scheme summarized above and explained thoroughly by Prucha et al. (1999). $\mathbf{A}$ is a regularization operator. ϵ controls the strength of the regularization.

The first part can be thought of as the "data fitting goal", meaning that it is responsible for making a model that is consistent with the data. The second part is the "model styling goal", meaning that it allows us to impose some idea of what the model should look like using the regularization operator $\mathbf{A}$. The model styling goal helps to keep the solution from diverging due to the null space in $\mathbf{L}$.

We can reduce the necessary number of iterations by preconditioning the model. This incorporates the preconditioning transformation $\mathbf{m} = \mathbf{A^{-1}p}$ (Fomel and Claerbout, 2002) into Equation (5). $\mathbf{A^{-1}}$ is obtained by mapping the multi-dimensional regularization operator $\mathbf{A}$ to helical space and applying polynomial division (Claerbout, 1998).

The question now is what to use for the regularization operator. We have chosen to make this operator a steering filter (Clapp, 2001) which will tend to create chosen dips. This abstract includes results from two different regularization schemes. One is called the "1-D regularization scheme" and simply tends to create dips horizontally along the offset ray parameter axis. The "2-D scheme" tends to create dips along chosen reflectors on the CMP axis and horizontally along the offset ray parameter axis.

RESULTS

We applied our regularized inversion scheme to a synthetic dataset provided to us by SMAART JV. This dataset is designed to have a significant shadow zone underneath the salt body. The result of wave-equation migration of this dataset can be seen in Figure 1. In the CMP-depth plane, note the severe decrease in amplitude of

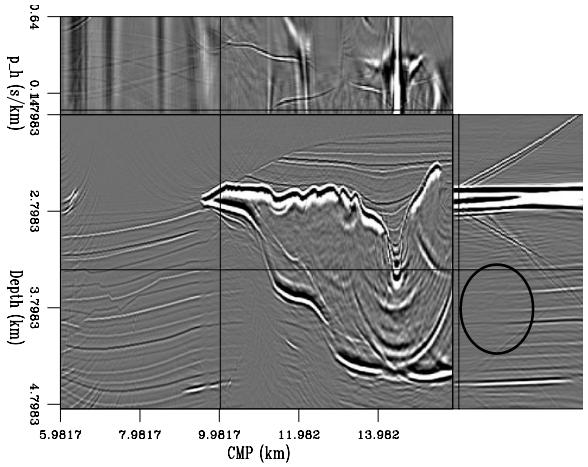

Figure 1: Result of angle-domain wave-equation migration. The oval on the offset ray parameter-depth plane indicates the "hole" described in Figure 2.

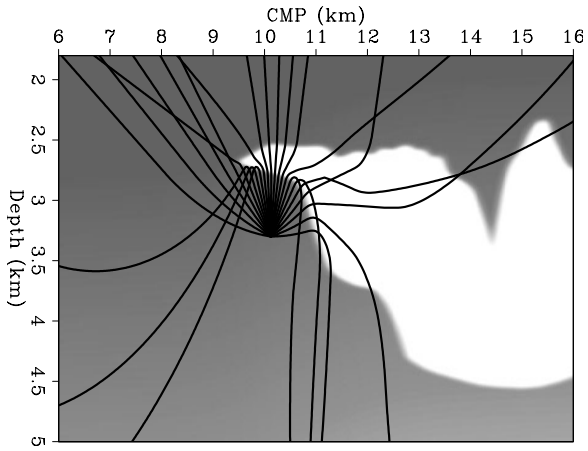

Figure 2: Demonstration of how a strong velocity contrast, such as salt, can cause a "hole" at a mid-range of angles. Rays generated by Huygen's wavefront tracing are overlaid on the velocity model.

the reflectors as they go beneath the salt. In the offset ray parameter (p_h)-depth plane, there is a large decrease in amplitude at small p_h. It is most visible inside the oval drawn on the figure. We consider this to be a "hole" in the event, since there is energy at very small p_h and large p_h. Figure 2 demonstrates how this occurs with ray tracing.

Figure 3 shows the result of 3 iterations of 1-D regularized inversion (Equation (5) with model preconditioning. Recall that the 1-D scheme tends to create dips horizontally along the p_h axis. The most obvious result of this is a substantial increase in the signal to noise ratio. In the context of this abstract, the more interesting result is the increase in strength of the events along the p_h axis. The "hole" that is circled in the p_h-depth plane is beginning to fill in. This in turn makes the reflectors in the CMP-depth plane appear to extend farther under the salt, with stronger amplitudes. This result is encouraging, but it seems likely that several more iterations would be necessary to really fill the hole.

To help fill in the shadow zones faster and since we can expect

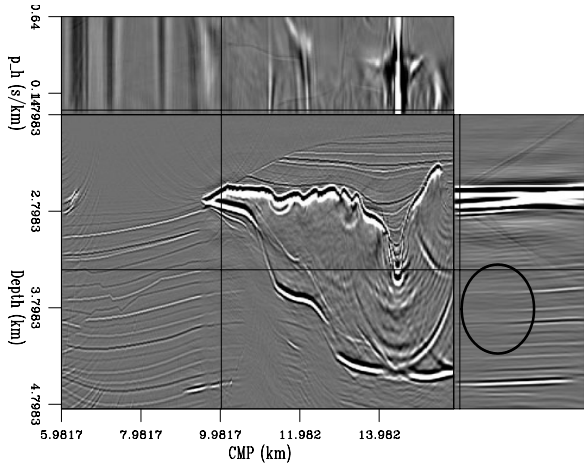

Figure 3: Result of 3 iterations of the 1-D regularized inversion with model preconditioning. Note the stronger events inside the oval indicating the "hole".

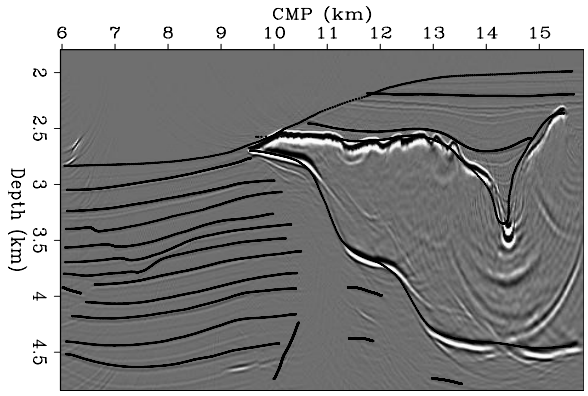

Figure 4: Migration result with picked reflectors for the 2-D regularized inversion overlaid.

continuity in spatial location as well as along p_hs, we used our 2-D regularization scheme. To do this, we first picked reflectors in the CMP-depth plane (Fig. 4) to be used to create the regularization operator in this dimension. In the inversion, this operator was cascaded with the operator that acts horizontally along the p_h axis.

The result of 3 iterations of the 2-D scheme can be seen in Figure 5. This result is smooth and very promising. The hole in the p_h axis is gone and the reflectors extended underneath the salt with a stronger amplitude. Unfortunately, this method also creates some obvious errors in the output image. The top of the salt has lost some of its features because the picked reflector there was not detailed enough. Also, the faults at the left side of the image have been smoothed out. In this case, neither of these areas are of particular interest and no real effort was made to prevent these errors.

Our regularization filter (**A**) smooths information over a limited distance. On the other hand, its inverse has effects over a large distance. As a result, preconditioning the model emphasizes the long wavelength features in early iterations, in this case smoothing along CMP and angle. The standard regularized approach solves for the short wavelength features at early iterations. One way to get the best of both approaches is to following the preconditioned model inversion with a standard regularized inversion. The result

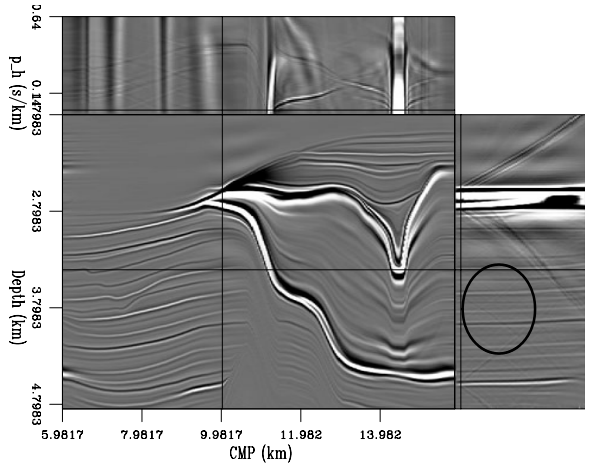

Figure 5: Result of 3 iterations of the 2-D regularized inversion with model preconditioning. Note the entire image is cleaner with strong events throughout the area enclosed by the oval.

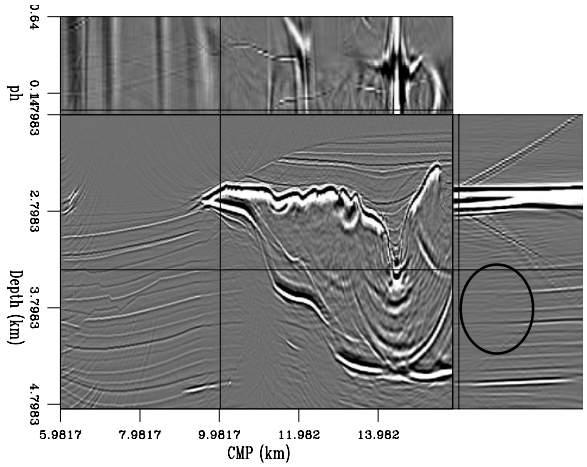

Figure 6: Result of 3 iterations of 2-D inversion with model preconditioning followed by 1 iteration of 2-D inversion without model preconditioning. Note the improvements beneath the salt nose and within the oval.

of 3 iterations of inversion with model preconditioning followed by one iteration of inversion without it can be seen in Figure 6. The result looks very similar to the migration result (Fig. 1). Many events containing higher frequencies have been revived, including some of the processing artifacts. However, close examination of the areas of particular interest reveals important differences.

In the CMP-depth plane, the reflectors going beneath the salt do not have the hole directly beneath the tip of the salt that is seen in the migration result. In the circled area in the p_h-depth plane, the reflectors are more constant in amplitude than in the migrated result. These improvements could be increased with more iterations of regularized inversion.

STEERING FILTER TEST

The results presented in this abstract are promising, but it is clear that the 2-D inversion is strongly dependent on the regularization operator. Since this operator is constructed from picked reflectors, it is important to know what happens if the reflector is not picked well. To examine this, we created a regularization operator from the "reflectors" picked in Figure 7. In this section, we will refer to the dips and reflectors from the migration result as "real" or "correct" and the dips and reflectors used for the inversion as "picked". There are several types of picked reflectors here:

Correct dip: The water bottom reflector has been correctly picked across the entire image.

No picked dips: The salt top and bottom have not been picked. There are no picked reflectors other than the water bottom in the right side of the image. This will force the inversion to use a regularization operator interpolated from other picked reflectors.

Opposite dips: The picked reflectors at the depths between 3 and 3.4 kilometers and 3.7 and 4.1 kilometers have dips opposite to the correct ones.

Similar dip: The picked reflector beginning at depth 3.75 km follows the correct dip for the most part, but ignores the slight change in dip at the fault at CMP position 7.2 km.

Crossing dips: Two picked reflectors cross each other at depth 4.5 km. This will test the stability of the inversion.

Reasonable dip in the shadow zone: The picked reflector beginning at depth 4.2 km follows the correct dip, but continues well into the shadow zone where it may or may not be correct, but is reasonable.

Unreasonable dip in the shadow zone: Also within the shadow zone is a completely absurd picked reflector put there to see if any event can be created.

The result of using this regularization operator for the 2-D inversion with model preconditioning is seen in Figure 8. As expected, the result doesn't look good at all. Looking specifically at the areas affected by the picked reflectors described above:

Correct dip: The water bottom was picked correctly and has lost no energy as seen in Figure 8.

No picked dips: The regularization in this area was dominated by the picked reflector along the water bottom. The only intact events related to the salt body are those with dips close to that of the water bottom. Some of the "nose" of the salt at depth 2.8 km and CMP location 10 km is visible despite having a dip opposite to the water bottom.

Opposite dips: The areas where the picked reflectors had a dip opposite to that of the real events, the energy of the events has been almost totally lost.

Similar dip: This event has kept its energy where the picked reflector followed it and across part of the faulted segment. Energy has been lost where the faulting caused the biggest difference in dip, at the beginning and end of the faulted segment.

Crossing dips: Once again the energy in this area has been reduced. This behavior indicates that the inversion can handle the opposing dips.

Reasonable dip in the shadow zone: This reflector is stronger and more continuous in the shadow zone. This is promising behavior.

Unreasonable dip in the shadow zone: Almost no energy has been created by this picked reflector.

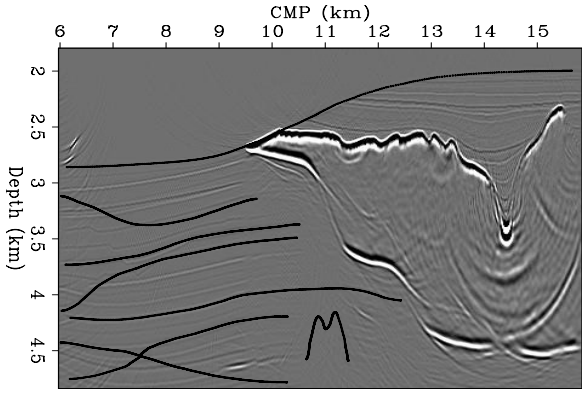

Figure 7: Migration result with the picked "reflectors" overlaid. These reflectors do not match the correct reflectors and should produce a bad result.

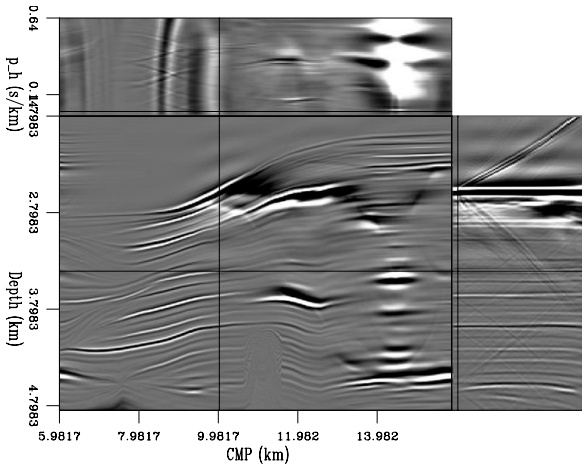

Figure 8: Result of 3 iterations of the 2-D regularized inversion with model preconditioning using badly picked reflectors.

CONCLUSIONS

This abstract has presented a wave-equation angle domain inversion scheme that uses steering filters as a regularization operator. These steering filters tend to create dips along chosen reflectors in the inversion result. We presented a 1-D scheme in which the steering filters simply acted horizontally along the p_h axis and a 2-D scheme in which the steering filters acting along the p_h axis was cascaded with steering filters acting along the dips of picked reflectors in the CMP-depth plane. Both of these methods increased the signal-to-noise ratio and helped to fill in the shadow zones.

We also examined the effect of the picked reflectors for the 2-D scheme. This was done by picking a variety of reflectors based on both the correct and the incorrect dips. This experiment showed that the inversion will reject dips that are incorrectly picked where data exists. This can even indicate areas where faulting has occurred. Picked dips that would generate an event that would interfere with the data are rejected. On the other hand, picked dips that generate an event that doesn't interfere with existing data are allowed. Picked dips that cross or meet at a point can be accommodated by the inversion. It is necessary to pick reflectors wherever the dominant dip changes.

ACKNOWLEDGMENTS

We would like to thank SMAART JV for the synthetic dataset used in our experiments and all of the sponsors of the Stanford Exploration Project for supporting us.

REFERENCES

Brandsberg-Dahl, S., de Hoop, M. V., and Ursin, B., 1999, The sensitivity transform in the common scattering-angle/azimuth domain:, *in* 61st Mtg. Eur. Assn. Geosci. Eng., Session:4053.

Claerbout, J., 1998, Multidimensional recursive filters via a helix: Geophysics, **63**, no. 5, 1532–1541.

Clapp, R. G., 2001, Geologically constrained migration velocity analysis: Ph.D. thesis, Stanford University.

Duquet, B., and Marfurt, K. J., 1999, Filtering coherent noise during prestack depth migration: Geophysics, **64**, no. 4, 1054–1066.

Fomel, S., and Claerbout, J., 2002, Multidimensional recursive filter preconditioning in geophysical estimation problems: submitted to Geophysics.

Geoltrain, S., and Brac, J., 1993, Can we image complex structures with first-arrival traveltime?: Geophysics, **58**, no. 04, 564–575.

Kuehl, H., and Sacchi, M., 2001, Generalized least-squares DSR migration using a common angle imaging condition: 71th Ann. Internat. Meeting, Soc. Expl. Geophysics, Expanded Abstracts, 1025–1028.

Mosher, C., and Foster, D., 2000, Common angle imaging conditions for prestack depth migration:, *in* 70th Ann. Internat. Mtg Soc. of Expl. Geophys., 830–833.

Nemeth, T., Wu, C., and Schuster, G. T., 1999, Least-squares migration of incomplete reflection data: Geophysics, **64**, no. 1, 208–221.

O'Brien, M. J., and Etgen, J. T., 1998, Wavefield imaging of complex structures with sparse point-receiver data: 68th Annual Internat. Mtg., Soc. Expl. Geophys., Expanded Abstracts, 1365–1368.

Prucha, M., Biondi, B., and Symes, W., 1999, Angle-domain common image gathers by wave-equation migration: 69th Ann. Internat. Meeting, Soc. Expl. Geophysics, Expanded Abstracts, 824–827.

Prucha, M. L., Clapp, R. G., and Biondi, B., 2000, Seismic image regularization in the reflection angle domain: SEP–**103**, 109–119.

Sava, P., Biondi, B., and Fomel, S., 2001, Amplitude-preserved common image gathers by wave-equation migration: 71th Ann. Internat. Meeting, Soc. Expl. Geophysics, Expanded Abstracts, 296–299.

Xu, S., Chauris, H., Lambare, G., and Noble, M., 2001, Common angle image gather - A strategy for imaging complex media: Geophysics, **66**, no. 6, 1877–1894.